

# Magnetic insulation of a space-charge dominated flow

A. Lahav,<sup>a)</sup> V. Berezovsky, and L. Schächter

*Department of Electrical Engineering, Technion-Israel Institute of Technology, Haifa 32000, Israel*

(Received 17 March 2003; accepted 30 June 2003)

We report experimental results of magnetic insulation of a space-charge dominated electron flow in a low energy vacuum diode with ferroelectric cathode. Although in the absence of the magnetic field the high current densities are measured well above the estimated space-charge limiting current, the diode is shown to be insulated by a relatively low magnetic field controlled primarily by the anode voltage. A model which accounts for the two-dimensional nature of the electrons flow in the diode has been developed and it reveals the microscopic picture of the flow. From the space-charge dominated vicinity of the cathode, electrons leave the small emitting area towards the large radius anode ring, along a trajectory that is parallel to the applied magnetic field. Only in the close vicinity of the anode plane, their trajectory bends towards the ring. Good agreement between the experimental data and theory was found. © 2003 American Institute of Physics.

[DOI: 10.1063/1.1602954]

## I. INTRODUCTION

More than a decade ago Gundel *et al.*<sup>1</sup> reported on strong electron emission from ferroelectric ceramics. This discovery was followed by extensive research<sup>2–4</sup> reporting various aspects of electron emission from ferroelectrics. In most cases, the research was motivated by finding an alternative emitter to be used in high-power microwave sources. A typical ferroelectric cathode consists of a ferroelectric “capacitor” with a uniform back electrode and a thin gridded one, facing the diode gap. Electron emission from the gridded surface follows the application of a triggering electric field of  $\sim 1 \times 10^6$  V/m and duration of 100–500 ns to the capacitor.

Basically, two different approaches have been adopted in order to explain the strong electron emission from ferroelectric cathode. The first approach focuses on variation of the internal properties of ferroelectric induced by an external field, while the second relies on electron emission from surface plasma formed on the gridded electrode.<sup>5,6</sup> The only quantitative model for strong electron emission from ferroelectric available to date was proposed by Schächter *et al.*<sup>7</sup> and it explains a wide variety of experimental data which was presented in Refs. 8 and 9. Moreover it has been shown theoretically that even when the ferroelectric is treated as a linear medium with a very high dielectric coefficient, strong electron emission is expected,<sup>10</sup> and high current densities above the space-charge limited current is feasible in a diode with a gridded dielectric cathode.<sup>11</sup>

Direct evidence of plasma formation on the surface of the ferroelectric cathode was given by observation of the plasma flashover with a fast charge-coupled device (CCD) camera<sup>12,13</sup> and by direct measurement of the ion and electron currents.<sup>14</sup> However the conclusive role of plasma on the electron dynamics in the diode gap is still to be determined. In fact several authors have shown experimentally

that the ferroelectric cathode governs the electron dynamics in the first few microseconds for diode gaps on the orders of 1 cm.<sup>9,15,16</sup>

The external triggering of the electron emission by a relatively low voltage is the main advantage of ferroelectric cathode over field emission sources. Other advantages include the availability of high total current and relatively low vacuum requirements. One of the main characteristics of ferroelectric emission at low anode voltages is that the measured current exceeds Child–Langmuir (CL) limiting current by several orders of magnitude.<sup>8,9,17</sup> It is important to emphasize that the CL limiting current is given only as a reference to the high current densities involved with strong electron emission from ferroelectric cathode, and by no means we consider the one-dimensional calculation of the limiting current to be valid in this case. We are contemplating to take advantage of this characteristic for construction of a low voltage (<1000 V) miniature coherent source of radiation. While the high currents associated with a low voltage ferroelectric emission guarantees high available power for radiation, the space-charge forces associated with this current may deteriorate the bunching process entailing considerably lower the conversion efficiency.

A possible solution for the bunching deterioration is using a cross field configuration. In a cross field device,<sup>18</sup> like the magnetron, a magnetic field is applied perpendicularly to the diode electric field. Above a certain value of the magnetic field ( $B_C$ ) the electrons are magnetically insulated from the anode. Drifting of the electrons towards the anode occurs only when the initially uncorrelated electrons, become bunched losing some of their energy to the radiation field. As energy is lost, electrons approach the anode where the radiation field is stronger thus enhancing the energy conversion. It is therefore possible that a low energy cross field oscillator based on a ferroelectric cathode will allow us to investigate the important trade-offs between a space-charge dominated beam and high conversion efficiency.

<sup>a)</sup>Electronic mail: lahav@tx.technion.ac.il

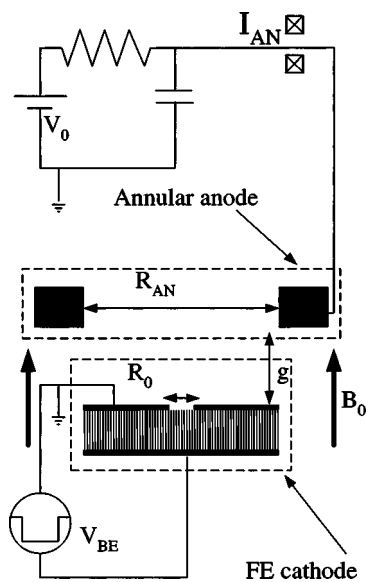


FIG. 1. Schematic of the experimental setup.

## II. EXPERIMENTAL SETUP

In this study we focus our attention to the quasistatic phenomenon in a cross-field diode with a ferroelectric cathode. Specifically, we have examined experimentally the magnetic insulation properties of the experimental setup which is illustrated in Fig. 1. The ferroelectric cathode consists of a ferroelectric “capacitor” made of commercially available (American Piezo Ceramic-“856” PLZT) ferroelectric ceramic disk; its diameter is 20 mm and its thickness is 1 mm. The capacitor’s back-electrode is uniform whereas the front electrode, i.e., the one facing the diode, has a single circular hole in the center; its diameter is 2 mm and the electrode’s thickness near the hole is less than 10  $\mu\text{m}$ .

The front electrode is grounded and electron emission is triggered by applying to the back electrode a 200 ns negative pulse. The pulse is generated by a 20  $\Omega$ -pulse forming network (Blumlein); its peak voltage is  $\sim 1.3$  kV. All signals were monitored for the first 2.5  $\mu\text{s}$ . An annular brass ring of 30 mm internal radius and 35 mm external radius located at a distance  $g$  ( $=4.5$  mm) forms the anode. Its center coincides with that of the front-electrode hole and it is connected to a 10 nF (low inductance  $<10$  nH) capacitor.

The pulsed axial magnetic field is generated by a pair of Helmholtz 12 cm diameter coils placed 6 cm apart along the setup axis—not shown in Fig. 1. Each coil consists of 40 turns of 1 mm wire wound around a Teflon core. The degree of uniformity of the magnetic field in the diode vacuum region was measured under dc conditions and found to be better than 96%. The coils are energized through a RC discharge circuit with a decay time of 1 ms. Since the diode metal parts may prevent full penetration of the magnetic field into the anode–cathode gap, the diode is triggered with a delay of at least 2 ms with respect to the discharge current in the coils. The magnetic field is determined based on measurement of  $I_L$  using a calibration curve prepared with a 1 kHz current-source. Both  $I_L$  and the diode current ( $I_A$ ) are measured with Pearson current-monitors.

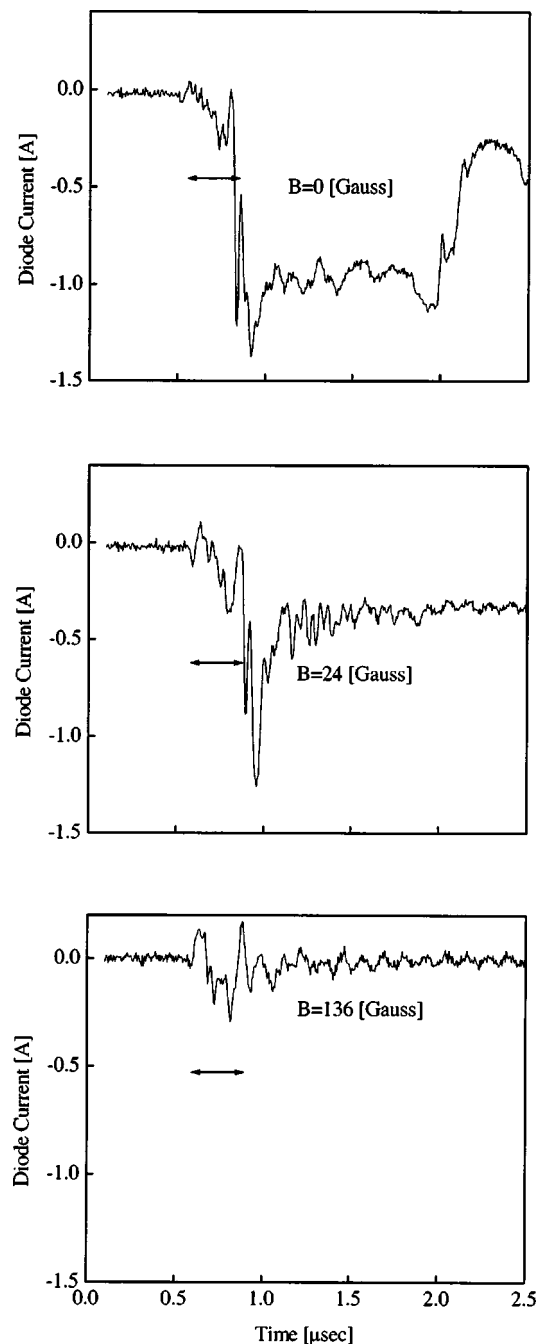


FIG. 2. The diode current for three different triggering events. The vertical dashed line denotes the start and end of the triggering back electrode pulse. The anode capacitor is charged to 370 V in all three events. Top frame:  $B = 0$  [Gauss]. Middle frame:  $B = 24$  [Gauss]. Bottom frame:  $B = 136$  [Gauss].

Vacuum levels are kept under  $5 \times 10^{-6}$  Torr. The back electrode voltage ( $V_{BE}$ ) and anode voltage ( $V_A$ ) are measured with standard Tektronix Probe. All data ( $V_A, V_{BE}, I_A, I_L$ ) are collected using a 500 MHz Tektronix oscilloscope (TDS640A).

## III. RESULTS AND DISCUSSION

Three different triggering events are illustrated in Fig. 2; in all three events the initial voltage on the anode capacitor is kept constant. In the case illustrated in the upper frame no axial magnetic field was applied whereas in the other two

frames the applied magnetic field was 24 and 136 G. The arrow indicates the start and end of the pulse that triggers the ferroelectric cathode. It clearly reveals that in the absence of axial magnetic field, current starts flowing in the diode immediately after the back-electrode is pulsed. A peak diode current of 1.2 A occurs about 250 ns after the back electrode voltage peaks. Similar delay of the current peak with respect to the back electrode triggering pulse has been observed in the past in both high and low energy experiments and has been explained in terms of the nonlinear response of the ferroelectric.<sup>7-9,17</sup> The diode current maintains levels around 1 A for at least 1000 ns after the peak value has been reached.

As in other experiments with low energy diodes operating with ferroelectric cathodes,<sup>8,17</sup> the measured currents in the absence of axial magnetic field are at least two orders of magnitude higher than the CL space-charge limited current which is estimated by using the well known one-dimensional law for a parallel plane diode. An estimate for the latter may be made by considering a pencil beam of radius 1 mm, spreading in 4.5 mm gap, between two electrodes charged to 370 V, the one-dimensional CL law gives current of approximately 3 mA. A better estimate taking into account the two-dimensional nature of an annular electron flow in the diode but ignoring the unique features of the ferroelectric emission has also been made entailing a current of 0.5 mA. Although the mathematical details are obviously different, both calculations predict current values that are at least two orders of magnitude smaller than the measured currents.

Applying an axial magnetic field by energizing the Helmholtz coils tends to reduce the anode current due to suppression of the radial motion. The middle frame of Fig. 2 shows that by applying magnetic field of 24 G, the diode current which follows the current peak has been reduced to levels around 0.5 A. In order to suppress the current peak, a larger magnetic field has to be applied as can be seen in the bottom frame where the diode current has vanished after applying more than five times the magnetic field (136 G). The oscillations which are observed in the diode current during the time which the back electrode pulse is active is probably due to quasioleostatic coupling in the setup.

Further investigation of the axial magnetic field effect on the diode current can be made by looking to the total charge flowing in the diode within the measurement time frame

$$Q_D = \int_0^{2.5 \mu\text{sec}} I_{\text{diode}}(t') dt'. \quad (1)$$

Figure 3 summarizes 59 experiments with identical initial anode voltage (370 V). Clearly, the dependence of the total charge flowing in the diode decreases with magnetic field and it reaches a minimum at approximately 80 G. However, the charge flowing in the diode does not vanish completely due to the coupling in the experimental setup combined with the nonlinearity of the diode. Nevertheless, after the first 200 ns the anode current is virtually zero—see bottom frame Fig. 2. Consequently, we consider the diode magnetically insulated above a cutoff of 80 G.

Based on the previous procedure, we determined the cut-off magnetic field ( $B_C$ ) for different values of initial anode

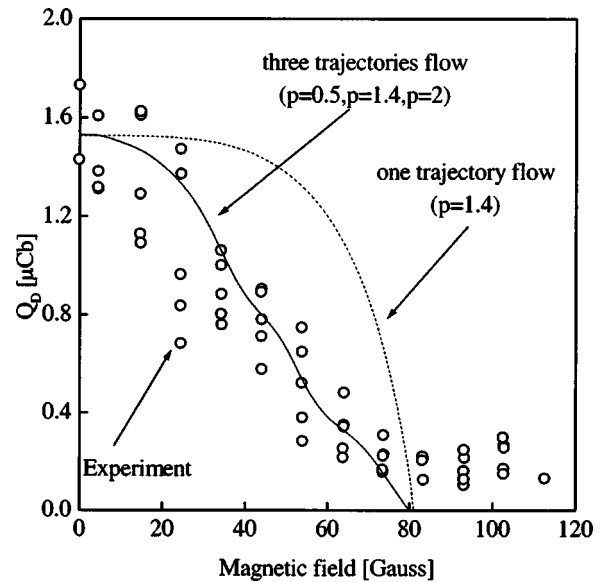


FIG. 3. The total charge flowing in the diode within measurement time-frame as a function of the magnetic field. Each circle corresponds to one triggering event where the anode capacitor is charged initially to 370. The dashed line is calculated from the model using trajectory with  $p=1.4$ . The solid line is calculated from the model using superposition between trajectories with  $p=0.5$ ,  $p=1.4$ , and  $p=2.0$ .

voltage. Figure 4 clearly shows a linear dependence between the square of the cutoff field and the initial anode voltage. This dependence of the cutoff field and the anode voltage raises the need for a comparison to the well known Hull cutoff condition. In the case of an infinite coaxial diode the Hull cutoff field is given by

$$B_c^2 = \left( \frac{8m}{e} \right) \frac{R_{AN}^2}{(R_{AN}^2 - R_C^2)^2} V_{AN} \quad (2)$$

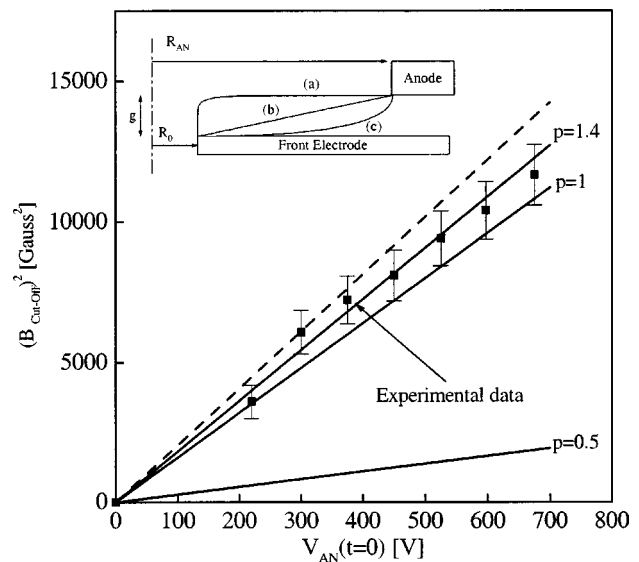


FIG. 4. The square of the cut-off field as a function of the anode voltage. Experimental points are denoted by squares. The coaxial diode (dashed line) is calculated using  $R_0=1$  mm,  $R_{AN}=15$  mm. The model lines are calculated using  $R_0=1$  mm,  $R_{AN}=15$  mm, and  $g=4.5$  mm. Inset frame: Three typical electron trajectories.

where  $m$  and  $e$  are electron's mass and charge respectively,  $R_{AN}$  and  $R_C$  are the anode and cathode radii, and  $V_{AN}$  is the anode voltage. The dashed line in Fig. 4 represents the expression in Eq. (2) using  $R_{AN}=15$  mm and  $R_0=1$  mm. This crude estimate of the cutoff field gives a reasonable match to the measured values in spite of the different geometries.

In what follows, it will be demonstrated that this result indicates that near the anode, electrons follow almost pure radial motion and their energy is given only by the voltage imposed by the anode ring. In the absence of a magnetic field the excess of current beyond the space-charge limiting current may be explained by local coupling of the energy from the ferroelectric capacitor into the diode gap.<sup>11</sup> In that case the electric field which is coupled from the cathode into the diode gap, is localized near the triple boundary between metal-ferroelectric and vacuum.<sup>10</sup> Hence, electrons will follow paths extending from the annular triple boundary at the cathode to the metallic edge of the anode ring—at this point the field is completely determined by the anode geometry and the anode voltage.

We developed a model which accounts for the two-dimensional nature of electron flow in the diode. Within the framework of this model we examined quasianalytically the effect of different electrons trajectories on the potential distribution in the diode gap. With the potential distribution established, it is possible to determine the diode impedance in the space-charge limiting regime as a function of the applied magnetic field. Increasing the latter, it is possible to reduce the current to zero—this is the cutoff field. In the framework of the model, the electrons trajectory may be described in a radial coordinate system by

$$\left(\frac{R-r}{R-R_0}\right)^p + \left(\frac{z}{g}\right)^p = 1, \quad (3)$$

where  $p$  defines the curvature of the trajectory. Three typical trajectories are shown in the inset of Fig. 4. Electrons in trajectory (a) start by moving vertically from the cathode and end with a pure radial motion ( $p \gg 1$ ); in trajectory (b) the electrons follow a straight line from the cathode to the anode ( $p=1$ ); in trajectory (c) electrons start by moving parallel to the anode and end moving vertically towards the anode ( $p < 0.5$ ). The full lines in Fig. 4 represent the square of the cutoff magnetic field calculated by the model for different anode voltages. The best fit with the experimental results is found to be with  $p=1.4$ , and for  $p > 2$  all lines fit the results that have been calculated for the infinite coaxial diode. The fact that the trajectory with  $p=1.4$  gives the best fit to the measured data, demonstrates that in a sufficiently *high magnetic field*, but still below cutoff, electrons traverse the diode parallel to the applied magnetic field and only in the close vicinity of the anode their motion becomes perpendicular to this field. Most importantly, this result indicates that plasma plays no role in the process since an applied magnetic field of few tens or 100 G has no significant effect on a plasma flow. This result also explains the good agreement of the coaxial theoretical result and our experiment. Up to the anode plane, electrons move parallel to the magnetic field gain-

ing only some small kinetic energy and only in the vicinity of the anode plane their motion becomes transverse exactly as in a coaxial configuration.

In spite of good agreement between the model and the experiment with regard to the cutoff field, when assuming  $p=1.4$  and applying a low intensity magnetic field (way below cutoff) the model overestimates the total charge that traverses the diode—see Fig. 3. For this reason we concluded that for low intensity magnetic field, electrons may follow several trajectories. And indeed, the model was extended to include three trajectories ( $p=0.5$ ,  $p=1.4$ , and  $p=2$ ) assuming that along each trajectory flows one third of the total current. The solid curve in Fig. 3 illustrates very good agreement between the prediction of the extended model and the experimental data.

Two important comments are in place now. First, the role of the ferroelectric cathode is to generate an intense electron cloud in the close vicinity of the cathode, enabling currents by far larger than would be “allowed” by the corresponding CL limiting current for the given geometry and anode voltage. Since inherently the CL limit includes energy conservation, the immediate concern would be the energy source that enables this high current. This topic has been discussed in the past<sup>7-9,17</sup> and it was shown that the excess of current is directly related to electrostatic energy coupled by the ferroelectric capacitor within the diode gap—typically in the close vicinity of the *cathode*. The current study indicates that this coupled energy has no direct impact on the insulation of this diode. This may be readily understood since our model shows that the main insulating process occurs in the close vicinity of the *anode*. Second, it is well known<sup>19,20</sup> within the framework of a one-dimensional (1D) theory, that close to cutoff the slope of the current (or charge) as a function of the magnetic field, becomes infinite. Our model confirms this result for  $p \geq 2$ . In fact, even for  $p=1.4$ , Fig. 3 shows a very high slope. In practice, because of the 2D character of the electron flow, the theoretical slope close to cutoff is significantly more moderate.

In conclusions, we have examined experimentally the magnetic insulation characteristics of a vacuum diode with ferroelectric cathode. This cathode is unique since it may provide currents by two orders of magnitude higher than CL limit for the same geometry and anode voltage. Electrostatic energy coupled from the ferroelectric capacitor in the diode gap is responsible to the excess of current. In spite the high currents the insulation, is still controlled only by the anode voltage and it is virtually unaffected by the energy coupled from the ferroelectric. A simple model that was briefly introduced here, helped clarify the physical picture of the flow in this diode. It demonstrated that while the ferroelectric and space-charge effects are dominating the phenomena in the close vicinity of the cathode, the insulation is determined by the magnetic field and the characteristics in the close vicinity of the anode.

## ACKNOWLEDGMENT

One of the authors (A.L.) wishes to thank Ya. E. Krasik for fruitful discussions regarding some experimental aspects of this study.

- <sup>1</sup>H. Gundel, H. Riege, E. Wilson, J. Handerek, and K. Zioutas, *Bull. Am. Phys. Soc.* **34**, 193 (1989).
- <sup>2</sup>H. Riege, *Nucl. Instrum. Methods Phys. Res. A* **340**, 8089 (1994).
- <sup>3</sup>C. B. Fleddermann and J. A. Nation, *IEEE Trans. Plasma Sci.* **25**, 212 (1997).
- <sup>4</sup>G. Rosenman, D. Shur, Ya. E. Krasik, and A. Dunaevsky, *J. Appl. Phys.* **88**, 6109 (2000).
- <sup>5</sup>G. Pleyber, K. Biedrzycki, and R. Le Bihan, *Ferroelectrics* **141**, 125 (1993).
- <sup>6</sup>H. Riege, *Nucl. Instrum. Methods Phys. Res. A* **340**, 80 (1994).
- <sup>7</sup>L. Schächter, J. D. Ivers, J. A. Nation, and G. S. Kerslick, *J. Appl. Phys.* **73**, 8097 (1993).
- <sup>8</sup>J. D. Ivers, L. Schächter, J. A. Nation, G. S. Kerslick, and R. Advani, *J. Appl. Phys.* **73**, 2667 (1993).
- <sup>9</sup>D. Flechtner, C. Golkowski, J. D. Ivers, G. S. Kerslick, J. A. Nation, and L. Schächter, *J. Appl. Phys.* **83**, 955 (1998).
- <sup>10</sup>L. Schächter, *Appl. Phys. Lett.* **72**, 421 (1998).
- <sup>11</sup>L. Schächter, D. Fletchner, Cz. Golkowski, J. D. Ivers, and J. A. Nation, *J. Appl. Phys.* **84**, 6528 (1998).
- <sup>12</sup>H. Riege, I. Boscolo, J. Handerek, and U. Herleb, *J. Appl. Phys.* **84**, 1602 (1998).
- <sup>13</sup>Ya. E. Krasik, A. Dunaevsky, and J. Felsteiner, *J. Appl. Phys.* **85**, 7946 (1999).
- <sup>14</sup>A. Dunaevsky, Ya. E. Krasik, J. Felsteiner, and S. Dorfman, *J. Appl. Phys.* **85**, 8464 (1999).
- <sup>15</sup>M. Miyake, S. Ibuka, K. Yasuoka, and S. Ishii, *Jpn. J. Appl. Phys., Part 1* **36**, 6004 (1997).
- <sup>16</sup>W. Zhang and W. Huebner, *J. Appl. Phys.* **83**, 6034 (1998).
- <sup>17</sup>A. Lahav, V. Berezovsky, and L. Schächter, *J. Appl. Phys.* **88**, 3202 (2000).
- <sup>18</sup>R. G. Hutter, *Beam and Wave Electrons in Microwaves Tubes* (Van Nostrand, Princeton, New Jersey, 1960).
- <sup>19</sup>L. Page and N. Adams, *Phys. Rev.* **69**, 492 (1946); L. Page and N. Adams, *ibid.* **69**, 494 (1946); L. Gold, *J. Appl. Phys.* **25**, 683 (1954).
- <sup>20</sup>Y. Y. Lau, P. J. Christensom, and D. Chernin, *Phys. Fluids B* **5**, 4486 (1993).